Control of dissected leaf morphology by a Cys(2)His(2) zinc finger transcription factor in the model legume *Medicago truncatula*

Jianghua Chen[a,1], Jianbin Yu[b,1,2], Liangfa Ge[a,1], Hongliang Wang[a,1,3], Ana Berbel[c], Yu Liu[a], Yuhui Chen[a], Guangming Li[a], Million Tadege[a,4], Jiangqi Wen[a], Viviane Cosson[d], Kirankumar S. Mysore[a], Pascal Ratet[d], Francisco Madueño[c], Guihua Bai[b], and Rujin Chen[a,5]

[a]Plant Biology Division, Samuel Roberts Noble Foundation, Ardmore, OK 73401; [b]US Department of Agriculture/Agricultural Research Service Hard Winter Wheat Genetics Research Unit, Manhattan, KS 66506; [c]Instituto de Biología Molecular y Celular de Plantas (IBMCP), Consejo Superior de Investigaciones Científicas, Universidad Politécnica de Valencia, CPI, Ed. 8E, Ingeniero Fausto Elio s/n, 46022 Valencia, Spain; and [d]Institut des Sciences du Végétal, Centre National de la Recherche Scientifique, 91198 Gif-sur-Yvette, France

Plant leaves are diverse in their morphology, reflecting to a large degree the plant diversity in the natural environment. How different leaf morphology is determined is not yet understood. The leguminous plant *Medicago truncatula* exhibits dissected leaves with three leaflets at the tip. We show that development of the trifoliate leaves is determined by the Cys(2)His(2) zinc finger transcription factor PALM1. Loss-of-function mutants of *PALM1* develop dissected leaves with five leaflets clustered at the tip. We demonstrate that PALM1 binds a specific promoter sequence and down-regulates the expression of the *M. truncatula LEAFY/UNIFOLIATA* orthologue *SINGLE LEAFLET1* (*SGL1*), encoding an indeterminacy factor necessary for leaflet initiation. Our data indicate that *SGL1* is required for leaflet proliferation in the *palm1* mutant. Interestingly, ectopic expression of *PALM1* effectively suppresses the lobed leaf phenotype from overexpression of a class 1 KNOTTED1-like homeobox protein in *Arabidopsis* plants. Taken together, our results show that PALM1 acts as a determinacy factor, regulates the spatial-temporal expression of *SGL1* during leaf morphogenesis and together with the LEAFY/UNIFOLIATA orthologue plays an important role in orchestrating the compound leaf morphology in *M. truncatula*.

compound leaf development | zinc finger transcription factor PALM1 | LFY/UNI/SGL1 | KNOXI | morphogenesis

Plant leaves are lateral organs initiated as a peg-like structure from the flank of the shoot apical meristem (SAM), a pluripotent structure that is capable of self-renewal. They can be simple, consisting of a single flattened blade subtended by a petiole, or compound (or dissected), consisting of multiple blade units known as leaflets. The class 1 Knotted1-like homeobox proteins (KNOXIs) are required to maintain indeterminacy of the SAM (1). During early development, *KNOXI* genes are down-regulated at the incipient leaf primordium at the periphery of the SAM (2). This down-regulation marks the site of primordia initiation and is permanent in developing primordia that lead to simple leaves. However, the *KNOXI* genes are transiently reactivated in leaf primordia in most eudicot species that have compound leaves, indicating a requirement for a transient phase of indeterminacy in the initiation of leaflet primordia at leaf margins during compound leaf development (3). However, the transient indeterminacy is not sufficient for compound leaf development, as it can also lead to simple leaves as a result of secondary morphogenesis in some plants (3). In some leguminous plants (Fabaceae) that belong to the inverted repeat lacking clade (IRLC), including garden pea (*Pisum sativum*) and alfalfa (*Medicago sativa*), the role of KNOXIs in maintaining indeterminacy is replaced by the FLORICAULA (FLO)/LEAFY(LFY) transcription factor UNIFOLIATA (UNI)/ SINGLE LEAFLET1 (SGL1) (4–6), because KNOXI proteins are not detected in leaves in the IRLC legumes (6). However, con-

flicting evidence exists to support the expression of *KNOXI* transcripts in leaves of IRLC legumes (7, 8). Recently, common molecular frameworks using NAM/CUC transcription factors and auxin gradients have been shown to play a role in compound leaf development in diverse species (9–12). Leguminous plants belong to the third largest family of flowering plants with significant economic value (13). Leaves of many leguminous species are pinnate, palmate, or higher-ordered compound. However, how different leaf morphology is determined in legumes is not yet understood.

Results

Isolation and Characterization of *palmate-like pentafoliata1* Mutants. To identify additional regulators of leaf morphogenesis in legumes, we screened a mutant collection in the model legume *Medicago truncatula* (cv. Jemalong A17) derived from fast neutron bombardment deletion mutagenesis and isolated two leaf mutants, M469 and M534. Mature leaves developed in these two mutants are palmate-like pentafoliate in contrast to the trifoliate WT leaves (Fig. 1 *A–E*). We named these mutants *palmate-like pentafoliata1-1* (*palm1-1*) and *palm1-2*. Compared with WT compound leaves, which have a terminal and two lateral leaflets (LLs), mature leaves in the *palm1* mutants have a terminal and two pairs of LLs clustered at the tip of the petiole. In addition, the two distally oriented LLs (LLd) are subtended by rachis structures similarly as the terminal leaflet (TL; Fig. 1 *B–E*). SEM and histochemical analysis show the presence of elongated epidermal cells at the surface and three vascular bundles, with two on the adaxial side of the rachis structures, indicating changes of LLd to the TL morphology in the *palm1* mutant (Fig. 1 *H, I, M,* and *N* and Fig. S1).
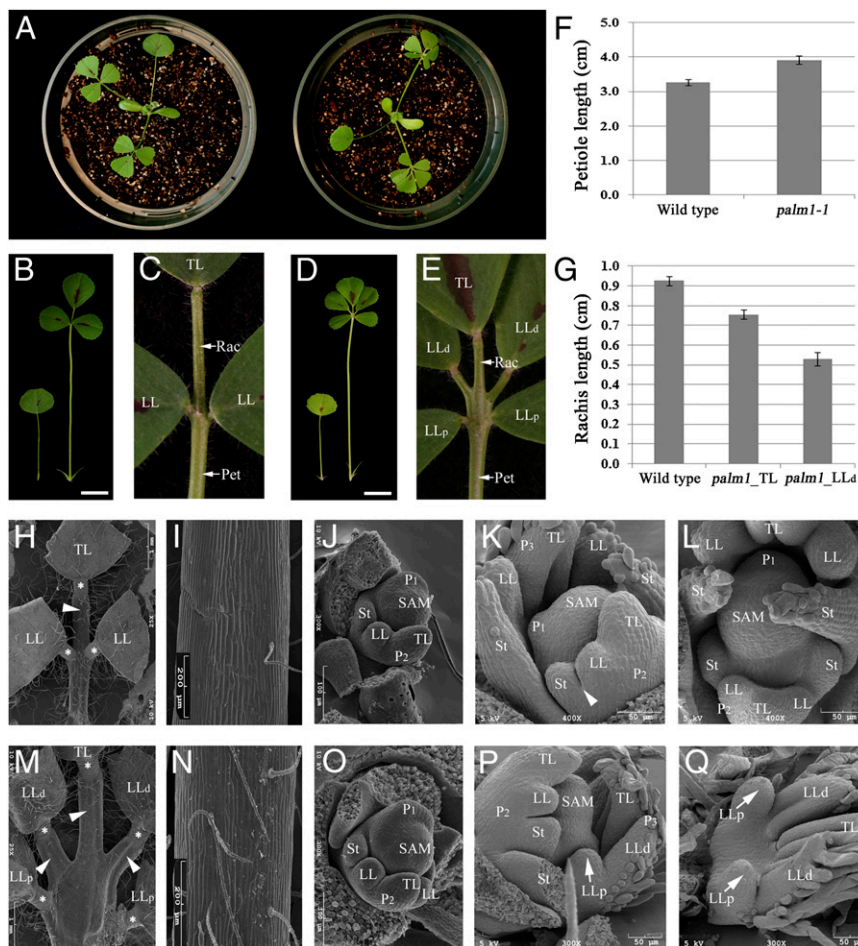
Fig. 1. *M. truncatula palm1-1* mutant exhibits altered leaf form: (*A*) 3-wk-old WT (Jemalong A17; *Left*) and *palm1-1* mutant (*Right*); (*B*) juvenile (*Left*) and compound (*Right*) leaves of WT plant; (*C*) high-magnification view of *B*; (*D*) juvenile (*Left*) and compound (*Right*) leaves of the *palm1-1* mutant; and (*E*) high-magnification view of *D*. (*F*) Measurements of the petiole length of compound leaves on the fifth node of 6-wk-old WT and *palm1-1* mutant plants. (*G*) Measurements of the rachis length of compound leaves. Shown are means ± SE (*n* = 10; *F* and *G*). (*H–Q*) SEM images of compound leaves (*H* and *M*), rachis (*I*, *N*; arrowheads in *H* and *M*), and leaf primordia at different developmental stages (*J–L*; *O–Q*) of WT (*H–L*) and the *palm1-1* mutant (*M–Q*). Asterisks in *H* and *M* indicating petiolules. Arrowhead in *K* indicates the boundary between St and LL. Arrows in *P* and *Q* indicate LLp developed in the P$_3$ primordia. P, Plastochron; Rac, rachis; Pet, petiole. (Scale bars, 1 cm in *B* and *D*.)

Accompanying these changes, the *palm1* mutants also exhibit alterations in the proximal-distal axis of compound leaves. Compared with WT leaves, the petiole length of mature leaves in 6-wk-old *palm1-1* mutant was increased by approximately 20% (Fig. 1*F*). Conversely, the length of the central rachis was reduced by approximately 19%, although rachis structures were developed on LLd in the mutant (Fig. 1*G*).

We attempted to identify the earliest morphological alterations during leaf development in the *palm1* mutant using SEM. In WT plants, leaf primordia after initiation (P$_0$ for Plastochron 0) from the periphery of the SAM developed a pair of stipule (St) primordia at P$_1$, a pair of LL primordia, boundaries between St and LL, and LL and TL at P$_2$, and the differentiation of TL and St as indicated by trichomes developed on their abaxial surface at P$_3$ (5) (Fig. 1 *J–L*). Leaf development progressed normally in the *palm1-1* mutant until the P$_3$ stage, when a pair of extra leaflet primordia, the proximally oriented LL (LLp), developed at the base of LLd, which were initiated at the P$_2$ stage (Fig. 1 *O–Q*; arrows). The earliest morphological alteration in the *palm1* mutant, the development of extra leaflet primordia in a basal position, suggest that *PALM1* plays a key role in the suppression of the morphogenetic activity in the proximal region of the compound leaf primordium, which is required to maintain the trifoliate morphology of compound leaves and the morphology of LL without the rachis structure in WT plants.

PALM1 encodes a Cys(2)His(2) zinc finger transcription factor. By using a map-based approach, we mapped the *PALM1* locus to a 45-kb interval on chromosome 5 (Fig. 2 *A–C*; Table S1 and Figs. S2 and S3). There are eight annotated ORFs in this genomic interval that are deleted in both *palm1-1* and *palm1-2* mutants (Fig. 2*D*). Three show syntenic relationships with *Arabidopsis thaliana* homologues on chromosome 4 (Table S2). To test which ORF is the candidate gene, we first screened two other mutant collections and isolated four mutants with the same phenotype as the original *palm1-1* and *palm1-2* mutants. We named these additional mutants *palm1-3, -4, -5,* and *-6* (Table S3). Sequence analysis indicates that *palm1-3* carries a 26-bp deletion between positions 243 and 269, and *palm1-4, palm1-5,* and *palm1-6* carry tobacco *Tnt1* retrotransposons at positions 114, 302, and 583, respectively, within the coding region of ORF3 (Table S3). Second, introducing the WT ORF3 locus, including 2.718-kb 5′-flanking sequence, 0.756-kb ORF, and 1.028-kb 3′-downstream sequence, into the *palm1-1* mutant rescued the mutant phenotype (Fig. 2*E*). Based on these results, we conclude that *PALM1* corresponds to ORF3, an intron-less gene that encodes a small protein of 251 aa.

Sequence comparison indicates that PALM1 and its close homologues from other plant species share syntenic chromosomal locations and are highly conserved in the EPF-type Cys(2)His(2) zinc finger DNA-binding domain at their N-termini (14) and in the EAR repressor domain identified in the class II ERF transcriptional repressors at their C-termini (15) (Fig. 2*F* and Fig. S4). Furthermore, PALM1 and its homologues from closely related legume species such as alfalfa (*M. sativa*), *Lotus japonicus*, and soybean (*Glycine max*) share a higher degree of sequence similarity than those from more distantly related species such as *A. thaliana* (Fig. 2*F* and Fig. S4). However, the role of these homologous genes is still not yet known.
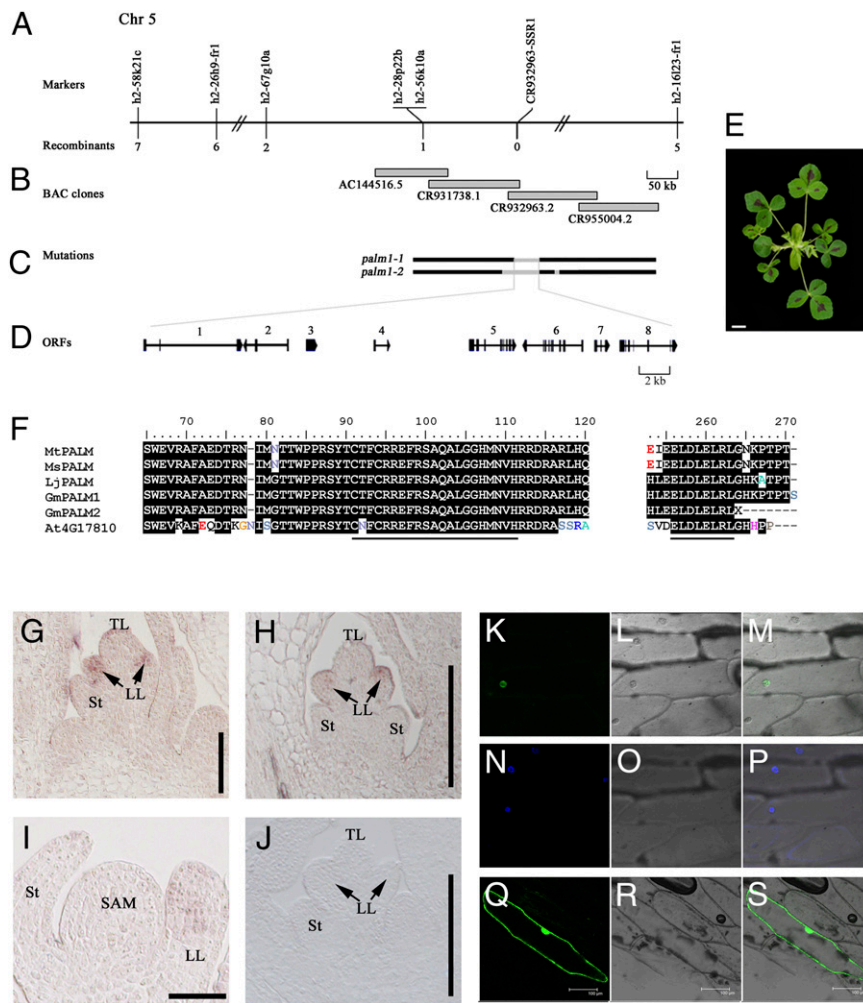
Fig. 2. Map-based cloning and characterization of *PALM1*. (*A*) *palm1* was mapped to contig 77 of chromosome 5 closely linked to the CR932963-SSR1 marker. Top shows markers that cosegregate with *palm1*; bottom shows number of recombinants. (*B*) Bacterial artificial chromosome clones in the region. (*C*) Deletion borders identified in *palm1-1* and *palm1-2* mutants using chromosomal walking. (*D*) Eight ORFs annotated within the deleted region in *palm1-1* and *palm1-2* alleles. Solid boxes/vertical lines denoting exons and horizontal lines denoting introns. (*E*) Introducing a plant transformation vector pCAMBIA3300-PALM1 that contains 2.718-kb 5′-flanking sequence, 0.756-kb ORF, and 1.028-kb 3′-downstream sequence of *PALM1* into the *palm1-1* mutant rescued the mutant phenotype. (*F*) Sequence alignments of conserved C_2H_2 zinc finger domain and EAR transcription repressor domain of *PALM1* with its homologues from alfalfa (*M. sativa*), *L. japonicus*, soybean (*G. max*), and *A. thaliana*. (*G-J*) RNA in situ hybridization. (*G* and *H*) Representative longitudinal sections of compound leaf primordia in 3-wk-old vegetative shoot apices used to detect *PALM1* transcripts in LL primordia (arrows; *G* and *H*) at the P_2 stage. (*I*) A longitudinal section of a vegetative shoot apex showing *PALM1* transcripts in LL. (*J*) A sense probe used as a negative control (arrows indicate LL). (*K–M*) Nuclear localization of 35S::GFP-PALM1 fusion protein detected in onion epidermal cells. (*N–P*) Nuclei stained by DAPI. (*Q–S*) Subcellular localization of 35S::GFP as a control. (*K*, *N*, and *Q*) Laser confocal images of GFP; (*L*, *O*, and *R*) DIC images of onion epidermal cells; and (*M*, *O*, and *S*) merged images. (Scale bars, 1 cm in *F*; 100 μm in *G–S*.)

Expression Pattern of *PALM1* and Subcellular Localization of the Encoded Protein. The tissue-specific expression of *PALM1* was analyzed by ways of in silico expression (16) and RNA in situ hybridization. The microarray-based expression analysis indicates that *PALM1* transcripts are expressed in vegetative shoot buds, leaves, and developing seeds, but remain low or hardly detectable in other tissues including roots, petioles, stems, flowers, pods, and the seed coat (Fig. S5). RNA in situ hybridization using a series of longitudinal sections of vegetative shoot apices shows that *PALM1* transcripts were detected in the LL primordia as early as the P_2 stage (Fig. 2 *G–I*; arrows). *PALM1* transcripts remained low or were barely detected in other tissues including SAM, TL, and stipules (Fig. 2 *G–I*). A sense probe, serving as a negative control, did not give any hybridization signals (Fig. 2*J*). Subcellular localization prediction, using Plant-PLoc (http://www.csbio.sjtu.edu.cn/cgi-bin/PlantPLoc.cgi), suggests that PALM1 is likely localized to nuclei. To verify this, we transiently expressed a GFP-PALM1 fusion protein driven by the constitutive Cauliflower Mosaic Virus 35S promoter in onion epidermal cells. Fig. 2 *K–S* shows that the fusion protein was specifically localized to nuclei, consistent with its predicted role as a transcription factor.

PALM1 Negatively Regulates *SGL1* Expression. Previously, we had shown that loss-of-function mutations in the *M. truncatula FLO/LFY/UNI* orthologue *SGL1* completely abolished the initiation of LL primordia at the P_2 stage, resulting in simple leaves (5). *SGL1* is expressed in both SAM and entire leaf primordia (5), the latter of which is partially overlapping with *PALM1* (Fig. 2 *G–I*). However, *SGL1* expression is greatly reduced in expanding leaflets (5). We hypothesized that *SGL1* may be required for the proliferation of LL in the *palm1* mutant. Quantitative RT-PCR data reveal that the *SGL1* transcript level was increased by 2.7-fold in vegetative shoot apices in the *palm1-1* mutant compared with WT (Fig. 3*A*). To further test whether the increase in the *SGL1* expression is simply caused by an increase in the number of leaflet primordia or an alteration in the expression pattern in the *palm1* mutant, we compared the expression of the *SGL1*pro::*uidA* (*GUS*) reporter gene in WT and in *palm1-1* mutant. Fig. 3*B* shows that in *palm1-1* mutant plants the *SGL1*pro::*uidA* reporter gene was expressed in all five leaflets, and its expression remained at a high level in expanding leaflets. In contrast, as previously reported, the same reporter gene was expressed in only the SAM and young leaflets, and its expression was greatly reduced in expanding leaflets in WT (5) (Fig. 3*C*). These results indicate that the loss-of-function mutation in *PALM1* up-regulated and expanded the spatial-temporal expression of *SGL1*, a positive regulator of leaflet initiation in *M. truncatula* (5).

To genetically test the involvement of *SGL1* in the proliferation of LL primordia in the *palm1* mutant, we generated *palm1-3 sgl1-1* double mutants (single mutant alleles all from the R108 ecotype). All leaves that developed in the double mutants were simple, similar to those in the *sgl1* single mutant (Fig. 3*D*), indicating an epistatic interaction between *sgl1* and *palm1*. The genetic interaction data support the requirement of *SGL1* in the proliferation of LL primordia in the loss-of-function *palm1* mutant.

Chen et al.

To further elucidate potential mechanisms that underlie *PALM1* regulation of *SGL1* expression, we took several approaches. We first ectopically expressed the *M. truncatula PALM1* gene under control of the constitutive 35S promoter in *A. thaliana* (Col-0) plants and then introduced the transgene (*35S::PALM1*) into the plant, through genetic crosses, that carries the *SGL1pro::GUS* reporter gene (5). Ectopic expression of *PALM1* did not affect the simple leaf morphology and flower development of the transgenic plants (Fig. 3 *E* and *F*), but it almost completely abolished the *SGL1pro::GUS* gene expression in leaves as indicated by quantitative RT-PCR and GUS staining data (Fig. 3 *E–G*), indicating that ectopic expression of *PALM1* suppresses the *SGL1* promoter activity in *A. thaliana* leaves.

Next, we used an electrophoretic mobility shift assay (EMSA) to determine the ability of PALM1 to bind the *SGL1* 5′-flanking sequence. The results indicate that PALM1 bound only sequences within the nucleotide region between −354 and −747 upstream of the translation initiation codon (Fig. S6). In addition, the interaction was abolished in the presence of high molar ratios of unlabeled specific competitor or the ion chelator EDTA (Fig. S6). Furthermore, by using a series of deletions, we narrowed the region in the *SGL1* 5′-flanking sequence that interacts with PALM1 to a 152-bp sequence between nucleotides −596 and −747 (Fig. 3 *H* and *I*). We further show that this interaction is specific, because (*i*) it was out-competed by unlabeled specific sequence, but not by a nonspecific sequence from a different region of the promoter; (*ii*) this interaction was not due to the His tag present in the fusion protein; and (*iii*) a smaller 80-bp deletion sequence lost the binding activity (Fig. 3*J*). Collectively, these results indicate that PALM1 may negatively regulate *SGL1* expression by directly binding its promoter sequence.

PALM1 Antagonizes the KNOXI Protein, KNAT1, in *A. thaliana*. In tomato plants, *KNOXI* genes are initially down-regulated at the incipient sites of leaf primordia (i.e., P_0) at the periphery of the SAM and subsequently reactivated in the developing leaf primordia to promote indeterminacy for compound leaf development (17–20). Depending on the developmental context, ectopic expression of *TKN*s, tomato *KNOXI* genes, has different effects on leaf shape, supporting a role for *TKN*s in stage-specific sup-

pression of leaf maturation in tomato (20). The KNOXI protein, kn1, has been postulated to play a role in the establishment of the proximal-distal polarity in maize (*Zea mays*) leaves (21). In *A. thaliana*, a plant with simple leaves, ectopic expression of an *A. thaliana KNOXI* gene, *KNAT1/BP*, leads to excessive lobing of leaf margins and uneven growth of laminae (20, 22–24) (Fig. 4*A*). To test the ability of *PALM1* to suppress the effects of overexpression of *KNAT1*, we made double transgenic lines, through genetic crossing, that ectopically express both *PALM1* and *KNAT1* (*35S::PALM1 35S::KNAT1*). We show that both leaf lobing and lamina outgrowth were completely abolished in the double transgenic lines (Fig. 4 *B* and *C*). Quantitative RT-PCR data show that the *KNAT1* transcript level was only slightly reduced in the double transgenic lines compared with the *35S::KNAT1* lines, in line with the transgene being driven by the constitutive 35S promoter. However, these results suggest that PALM1 may suppress the effects of overexpression of KNAT1 by regulating its downstream targets, instead of its transcription, in *A. thaliana* (Fig. 4*D*). Although KNOXI proteins are not detected in compound leaves in the IRLC legumes (6), these results are reminiscent of the previous observation that compound leaf development in IRLC legumes can still respond to ectopic expression of *KNOXI* genes (6) and suggest that PALM1 is capable of regulating leaf morphogenetic processes that are sensitive to the *KNOXI* regulation.

Discussion

Mature leaves in *M. truncatula*, an IRLC legume, are dissected with three leaflets at the tip. Previous studies have shown that the initiation of two LL primordia is controlled by the *M. truncatula LFY/UNI* orthologue *SGL1* (5) (Fig. 3*D*). In this study, we show that the *M. truncatula PALM1* gene encodes a Cys(2)His(2) zinc finger transcription factor and is required to maintain the trifoliate morphology of mature leaves. Several striking phenotypic changes in loss-of-function *palm1* mutants, development of two extra leaflets in a basal position, development of the rachis structure on two distally oriented LLs and alteration of the petiole and rachis length, suggest that *PALM1* suppresses the morphogenetic activity in developing leaf primordia and serves as a determinacy factor for leaf morphogenesis in *M. truncatula* (Fig. 1).

Fig. 3. *PALM1* and *SGL1* interaction. (*A*) Quantitative RT-PCR analysis of the *SGL1* expression relative to the expression of *MtActin2*. The level of *SGL1* transcripts was increased by 2.7-fold in *palm1-1* mutant compared with WT plants 3 wk after germination. Shown are means ± SE (*n* = 3). (*B*) GUS activity staining of 3-wk-old *M. truncatula palm1-1* mutant harboring the *SGL1pro::uidA* (*GUS*) reporter gene. GUS was expressed in the SAM and young and expanding leaflets. (*C*) The same reporter gene was expressed in the SAM and young leaflets, but not in expanding leaflets (arrow) in WT. (*D*) Compound leaf phenotype of *palm1-3 sgl1-1* double mutants. Shown from left to right are mature compound leaves of WT, *palm1-3*, *sgl1-1*, and *palm1-3 sgl1-1* mutants (all in the R108 ecotype). Leaves of the double mutants were simple, similar to those of the *sgl1* mutant, indicating an epistatic interaction between *sgl1* and *palm1*. (*E*) The *SGL1pro::uidA* reporter gene expressed in the SAM and rosette leaves of 3-wk-old WT *A. thaliana* plants. (*F*) The expression of the reporter gene was greatly suppressed in *35S::PALM1* plants. (*G*) Quantitative RT-PCR analysis of the reporter gene expression. The level of *GUS* transcripts was greatly reduced in *35S::PALM1 SGL1pro::GUS* plants compared with *SGL1pro::GUS* plants. Shown are means ± SE (*n* = 3). (*H*) Schematic drawing of the *SGL1* promoter including F1, F2, and F3 sequences upstream from the translation initiation codon and a series of deletion fragments of the F2 sequence. (*I*) EMSA of the F2 deletion sequences labeled with biotin in the presence and absence of purified His-tagged PALM1. (*J*) EMSA of the F2-3 sequence. Tested were the unlabeled F2-3 sequence in 10-, 20-, and 50-fold excess relative to the biotin-labeled sequence as specific competitors (indicated by +, ++, and +++), unlabeled F3-1 sequence in 50-fold excess as a nonspecific (NS) competitor, and His-tagged tobacco etch virus protease (TEV), an unrelated protein as a negative control. Arrows indicate shifted bands. (Scale bars, 1 cm in *B–D*.)
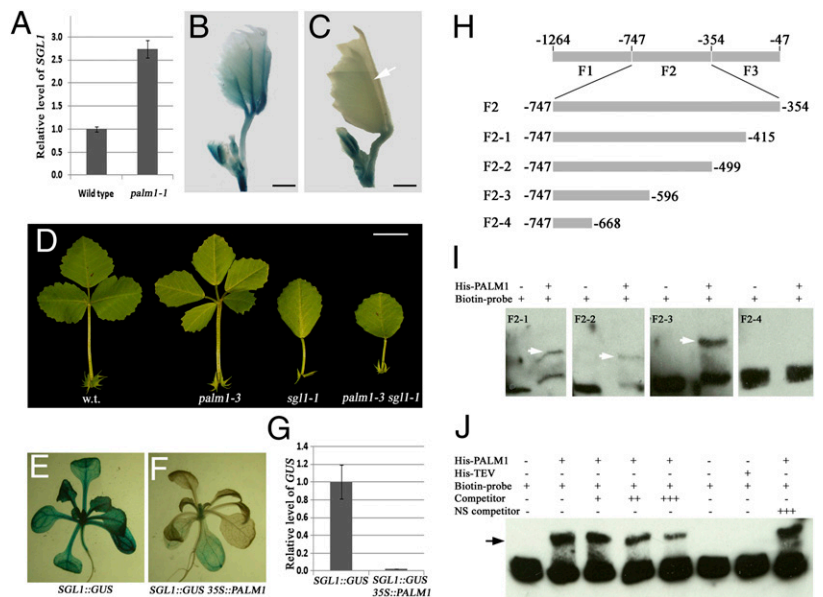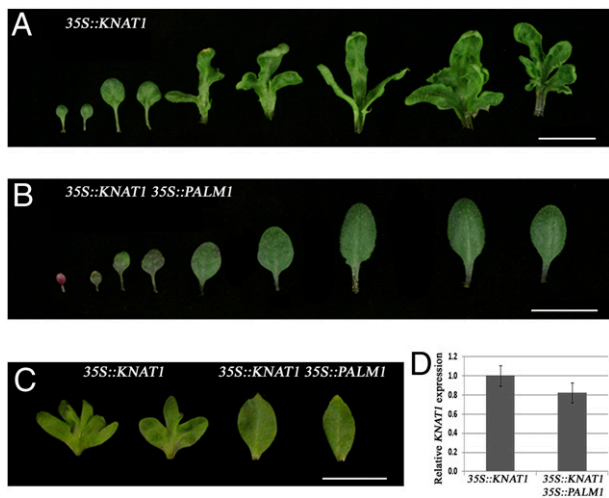
Fig. 4. *PALM1* and *KNAT1* interaction. (*A*) Rosette leaves of *35S::KNAT1Arabidopsis thaliana* plants. The fifth and older leaves were deeply lobed and outgrown. (*B*) Rosette leaves of *35S::KNAT1 35S::PALM1 A. thaliana* plants. Ectopic expression of *PALM1* completely suppressed *KNAT1*-induced lobing of leaf margins and the uneven outgrowth of the laminae. (*C*) Cauline leaves of *35S::KNAT1* plants (two on the left) and *35S::KNAT1 35S::PALM1* plants (two on the right). Similarly, *KNAT1*-induced leaf lobing and outgrowth of cauline leaves were suppressed by ectopic expression of *PALM1*. (*D*) Quantitative RT-PCR analysis of *KNAT1* expression relative to the level of *AtEF1a* expression. The level of *KNAT1* transcripts was only slightly reduced by the ectopic expression of *PALM1*. (Scale bars, 1 cm.)

Cys(2)His(2) zinc finger transcription factors are one of the largest families of transcription factors in plants (25, 26). Homologous sequences exist in lower land plants, suggesting an ancient origin and divergent function of these transcription factors. A similar situation also exists in mammals, in which a large increase in the diversity of Cys(2)His(2) zinc finger transcription factors is attributed to recent gene duplication and retraction (27). Recently, the tomato *LYRATE* gene, the orthologue of the *Arabidopsis JAGGED* (At1G68480) with five exons, has been shown to encode a Cys(2)His (2) zinc finger protein with an EAR domain at the N terminus, a C_2H_2 domain in the middle, and a Pro-rich motif at the C terminus (28). *LYRATE* appears to play a role in the outgrowth of lateral organs through modulation of the *KNOX* and auxin transcriptional networks in tomato (28). Outside of the Cys(2)His(2) domain, LYRATE and PALM1 do not share sequence similarities. In addition, *LYRATE* and *PALM1* do not share the same exon-intron structure as *PALM1* does not contain any introns. Thus, *PALM1* and *LYRATE* represent two distinct classes of Cys(2)His(2) zinc finger transcription factors. However, they both play a role in compound leaf development, albeit in different species.

Our results indicate that PALM1 binds a specific sequence in the promoter and negatively regulates the transcription of *SGL1*. Whereas *SGL1* is expressed in the SAM and the entire young leaf primordia (5), the expression of *PALM1* in LL primordia partly overlaps with that of *SGL1*. Consistently, the role of *PALM1* in the regulation of *SGL1* expression and leaf morphogenesis is more pronounced at late stages of leaf development as indicated by the up-regulation and expansion of *SGL1*pro::*GUS* reporter gene expression in expanding leaflets in the *palm1* mutant compared with WT (Fig. 3 *B* and *C*) and along the proximal-distal axis of leaves as indicated by the altered petiole and rachis length and the ectopic formation of rachis on LLs in the *palm1* mutants (Fig. 1). Our results support a model in which the negative regulator, *PALM1*, through its own spatial-temporal expression, defines the spatial-temporal expression of *SGL1* and the associated morphogenetic activity in leaf pri-

mordia, and through this regulation determines the trifoliate morphology of mature leaves (Fig. 5 *A–D*). In loss-of-function *palm1* mutants, the lack of the negative regulation resulting from loss of *PALM1* results in the up-regulation and expansion of *SGL1* expression and an increase in the morphogenetic activity, which leads to the development of extra leaflets at a basal position of leaves, ectopic formation of the rachis structure on the distally oriented LLs, and altered development of the proximal-distal axis of leaves (Fig. 5 *E* and *F*).

Taken together, our studies identify *PALM1* as a key regulator of dissected leaf morphogenesis in *M. truncatula*, an IRLC legume. Our analysis further shows that *PALM1* homologues exist in non-IRLC legumes including soybean and *L. japonicus* (Fig. 2*F* and Fig. S4), in which KNOXI proteins are expressed in leaves and likely associated with compound leaf development in these plants (6). Although functions of the *PALM1* homologues in these non-IRLC legumes are not yet known, it is tempting to speculate that they may be involved in compound leaf development in these plants through an antagonistic interaction with the KNOXI-mediated morphogenetic processes as suggested by the antagonistic interaction between PALM1 and KNAT1 in a heterologous system (Fig. 4). Alternately, *PALM1* homologues may have coevolved with the *FLO/LFY* orthologues in the IRLC legumes in which they regulate the FLO/LFY-type transcription factors during compound leaf development (6).

Methods

Plant Materials. Seeds of *M. truncatula* cv. Jemalong A17 (i.e., WT) were exposed to fast neutron radiation at a dosage level of 40 Gy and germinated in a greenhouse with a controlled environment. Approximately 30,000 M_2 plants derived from 5,000 M_1 lines were screened, resulting in the isolation of *palm1-1* (M469) and *palm1-2* (M534). Additional alleles in the *M. truncatula* R108 ecotype, *palm1-3* (GKB483), and *palm1-4* (NF1271), *palm1-5*
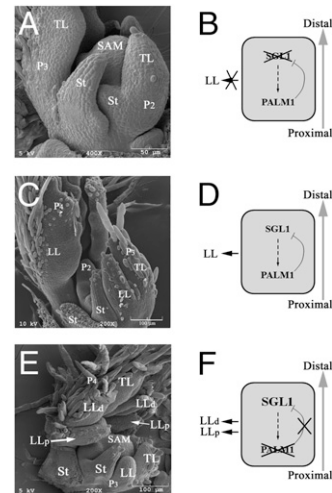

Fig. 5. Models of compound leaf development in *M. truncatula*. (*A* and *B*) Leaf development in the *single leaflet1* (*sgl1*) mutant. (*A*) SEM image of leaf primordia [adapted from Wang et al. (5)]. (*B*) A diagram of interactions between *SGL1* and *PALMATE-LIKE PENTAFOLIATA1* (*PALM1*). Loss of function of *SGL1* results in lack of formation of LL primordia and simple leaves. (*C* and *D*) Leaf development in WT plants. (*C*) SEM image of leaf primordia development. (*D*) A diagram of interactions between *SGL1* and *PALM1*. Dashed arrow indicates an epistatic genetic interaction between *SGL1* and *PALM1*. Distinct and partially overlapping spatial-temporal expression of *SGL1* and *PALM1* in leaf primordia and transcriptional repression of *SGL1* by *PALM1* define the morphogenetic activity at the leaf margin and the development of LL primordia and the trifoliate leaves. (*E* and *F*) Leaf development in the *palm1* mutant. (*E*) SEM image of leaf primordia development. (*F*) A diagram of interactions between *SGL1* and *PALM1*. Mutations in the *PALM1* gene up-regulate and expand the spatial-temporal expression of *SGL1* and result in an increased morphogenetic activity at the leaf margin and the development of LLd and LLp and pentafoliate leaves.

(NF227), and *palm1-6* (NF5022) were isolated from a collection of 1,400 T_2 T-DNA mutants (29) and a collection of 6,000 R_2 tobacco *Tnt1* retrotransposon mutants (30), respectively. *M. truncatula sgl1-1* mutant and *SGL1::uidA* transgenic lines (5) and *A. thaliana SGL1::uidA* (5) and *35S::KNAT1* (23) transgenic lines were as previously described. The *palm1-1* and *palm1-3* lines were backcrossed to their respective parental lines for three generations. BC_3 lines were used to characterize growth phenotypes.

Genetic Mapping. We generated F_2 mapping populations derived from crosses between *palm1-1* and *M. truncatula* cv. Jemalong A20 (*SI Methods*). The *PALM1* locus was identified using bulked segregant analysis, fine genetic mapping, and chromosomal walking (Table S1 and Figs. S2 and S3).

SEM. Shoot apices of 2- to 4-wk-old seedlings were subjected to vacuum infiltration in a fixative solution (5% formaldehyde, 5% acetic acid, 50% ethanol) for 30 min and then kept at room temperature overnight. SEM was carried out as described previously (5).

Subcellular Localization. Subcellular localization of PALM1 was determined using the coding sequence of GFP fused in-frame to the 5′-end of the coding sequence of PALM1 and transcribed from the Cauliflower mosaic virus 35S promoter. The resulting plasmid was bombarded into onion epidermal cells using a helium Biolistic device (PDS-1000; Bio-Rad). The GFP-PALM1 fusion protein was examined using a confocal laser scanning microscope (TCS SP2 AOBS; Leica). Primer sequences are listed in Table S4.

RNA in Situ Hybridization. RNA in situ hybridization was performed as previously described (31) with minor modifications. The *PALM1* probes correspond to a 300-bp sequence in the 3′-region of the *PALM1* mRNA. Ten-micrometer sections from shoot apices of 2- to 4-wk-old seedlings were processed and hybridized with digoxigenin-labeled sense and antisense probes.

Complementation and Ectopic Expression. For complementation studies, a genomic fragment, including 2.718-kb 5′-flanking sequence, 0.756-kb ORF, and 1.028-kb 3′-downstream sequence of *PALM1* was amplified by PCR and cloned into pGEM-T Easy vector (Promega). After sequence verification, the insert was digested with EcoRI and XbaI and subcloned into pCAMBIA3300. The resulting plasmid was introduced into *Agrobacterium tumefaciens* EHA105 strain by electroporation. For ectopic expression, a 756-bp genomic fragment containing the entire coding region of *PALM1* was amplified by PCR, digested with NcoI and BstEII and cloned into pCAMBIA3301. The resulting plasmid was introduced into *A. tumefaciens* EHA105 and GV3101 strains, and used to transform *M. truncatula* and *A. thaliana*, respectively. Primer sequences are listed in Table S4.

Stable Plant Transformation. *M. truncatula* and *A. thaliana* (*Col*-0) were transformed as previously described (5).

Quantitative RT-PCR. Total RNA samples were isolated from tissues using an RNeasy Plant Mini Kit (Qiagen). The quality of the RNA samples was determined by a Nanodrop Analyzer (BioMedical Solutions). Reverse transcription and cDNA synthesis were carried out with 2 μg of total RNA, using an Omniscript RT Kit (Qiagen) and oligo(dT)$_{15}$ columns. Real-time RT-PCR analysis was carried out as previously described (32). *M. truncatula Actin2* and *A. thaliana EF1a* were used as internal controls. Primer sequences are listed in Table S4.

***Escherichia coli* Expression and EMSA.** His(6)-tagged PALM1 was expressed in *E. coli* BL21 strain using pET32a vector and purified with the QIAexpressionist kit, following the manufacturer's instructions (Qiagen). EMSA was carried out with a Light Shift Chemiluminescent EMSA kit, following the manufacturer's instruction (Pierce). Briefly, we used 200 ng purified recombinant protein and 20 fmol biotin-labeled DNA fragment in a 20 μL reaction mix containing 10 mM Tris (pH 7.5), 50 mM KCl, 1 mM DTT, 2.5% glycerol, 0.05% Nonidet P-40, 5 mM MgCl$_2$, 0.5 mM EDTA, 5 ng/mL poly(dl•dC), and unlabeled DNA fragment at various molar ratios as competitors. Primer sequences are listed in Table S4.

1. Long JA, Moan EI, Medford JI, Barton MK (1996) A member of the KNOTTED class of homeodomain proteins encoded by the *STM* gene of Arabidopsis. *Nature* 379:66–69.
2. Hay A, Tsiantis M (2009) A KNOX family TALE. *Curr Opin Plant Biol* 12:593–598.
3. Bharathan G, et al. (2002) Homologies in leaf form inferred from *KNOXI* gene expression during development. *Science* 296:1858–1860.
4. Hofer J, et al. (1997) *UNIFOLIATA* regulates leaf and flower morphogenesis in pea. *Curr Biol* 7:581–587.
5. Wang H, et al. (2008) Control of compound leaf development by *FLORICAULA/LEAFY* ortholog *SINGLE LEAFLET1* in *Medicago truncatula*. *Plant Physiol* 146:1759–1772.
6. Champagne CE, et al. (2007) Compound leaf development and evolution in the legumes. *Plant Cell* 19:3369–3378.
7. Hofer J, Gourlay C, Michael A, Ellis TH (2001) Expression of a class 1 *knotted1*-like homeobox gene is down-regulated in pea compound leaf primordia. *Plant Mol Biol* 45:387–398.
8. Di Giacomo E, et al. (2008) Characterization of *KNOX* genes in *Medicago truncatula*. *Plant Mol Biol* 67:135–150.
9. Blein T, et al. (2008) A conserved molecular framework for compound leaf development. *Science* 322:1835–1839.
10. Koenig D, Bayer E, Kang J, Kuhlemeier C, Sinha N (2009) Auxin patterns Solanum lycopersicum leaf morphogenesis. *Development* 136:2997–3006.
11. Barkoulas M, Hay A, Kougioumoutzi E, Tsiantis M (2008) A developmental framework for dissected leaf formation in the Arabidopsis relative Cardamine hirsuta. *Nat Genet* 40:1136–1141.
12. Berger Y, et al. (2009) The NAC-domain transcription factor GOBLET specifies leaflet boundaries in compound tomato leaves. *Development* 136:823–832.
13. Graham PH, Vance CP (2003) Legumes: importance and constraints to greater use. *Plant Physiol* 131:872–877.
14. Takatsuji H (1999) Zinc-finger proteins: The classical zinc finger emerges in contemporary plant science. *Plant Mol Biol* 39:1073–1078.
15. Ohta M, Matsui K, Hiratsu K, Shinshi H, Ohme-Takagi M (2001) Repression domains of class II ERF transcriptional repressors share an essential motif for active repression. *Plant Cell* 13:1959–1968.
16. Benedito VA, et al. (2008) A gene expression atlas of the model legume *Medicago truncatula*. *Plant J* 55:504–513.
17. Janssen BJ, Lund L, Sinha N (1998) Overexpression of a homeobox gene, LeT6, reveals indeterminate features in the tomato compound leaf. *Plant Physiol* 117:771–786.
18. Parnis A, et al. (1997) The dominant developmental mutants of tomato, Mouse-ear and Curl, are associated with distinct modes of abnormal transcriptional regulation of a Knotted gene. *Plant Cell* 9:2143–2158.
19. Hareven D, Gutfinger T, Parnis A, Eshed Y, Lifschitz E (1996) The making of a compound leaf: Genetic manipulation of leaf architecture in tomato. *Cell* 84:735–744.
20. Shani E, et al. (2009) Stage-specific regulation of *Solanum lycopersicum* leaf maturation by class 1 KNOTTED1-LIKE HOMEOBOX proteins. *Plant Cell* 21:3078–3092.
21. Ramirez J, Bolduc N, Lisch D, Hake S (2009) Distal expression of knotted1 in maize leaves leads to reestablishment of proximal/distal patterning and leaf dissection. *Plant Physiol* 151:1878–1888.
22. Chuck G, Lincoln C, Hake S (1996) KNAT1 induces lobed leaves with ectopic meristems when overexpressed in Arabidopsis. *Plant Cell* 8:1277–1289.
23. Lincoln C, Long J, Yamaguchi J, Serikawa K, Hake S (1994) A *knotted1*-like homeobox gene in Arabidopsis is expressed in the vegetative meristem and dramatically alters leaf morphology when overexpressed in transgenic plants. *Plant Cell* 6:1859–1876.
24. Sinha NR, Williams RE, Hake S (1993) Overexpression of the maize homeo box gene, *KNOTTED-1*, causes a switch from determinate to indeterminate cell fates. *Genes Dev* 7:787–795.
25. Englbrecht CC, Schoof H, Böhm S (2004) Conservation, diversification and expansion of C2H2 zinc finger proteins in the Arabidopsis thaliana genome. *BMC Genomics* 5:39.
26. Takatsuji H (1998) Zinc-finger transcription factors in plants. *Cell Mol Life Sci* 54:582–596.
27. Tadepally HD, Burger G, Aubry M (2008) Evolution of C2H2-zinc finger genes and subfamilies in mammals: species-specific duplication and loss of clusters, genes and effector domains. *BMC Evol Biol* 8:176.
28. David-Schwartz R, Koenig D, Sinha NR (2009) LYRATE is a key regulator of leaflet initiation and lamina outgrowth in tomato. *Plant Cell* 21:3093–3104.
29. Scholte M, et al. (2002) T-DNA tagging in the model legume *Medicago truncatula* allows efficient gene discovery. *Mol Breed* 10:203–215.
30. Tadege M, et al. (2008) Large-scale insertional mutagenesis using the *Tnt1* retrotransposon in the model legume *Medicago truncatula*. *Plant J* 54:335–347.
31. Coen ES, et al. (1990) *floricaula*: A homeotic gene required for flower development in *Antirrhinum majus*. *Cell* 63:1311–1322.
32. Laxmi A, Pan J, Morsy M, Chen R (2008) Light plays an essential role in intracellular distribution of auxin efflux carrier PIN2 in *Arabidopsis thaliana*. *PLoS One* 3:e1510.

PLANT BIOLOGY